

# Mechanistic Study of Stress Relaxation in Urethane-Containing Polymer Networks

Jacob P. Brutman,<sup>†</sup> David J. Fortman,<sup>‡,§</sup> Guilhem X. De Hoe,<sup>†</sup> William R. Dichtel,<sup>\*,‡,§</sup> and Marc A. Hillmyer<sup>\*,†</sup>

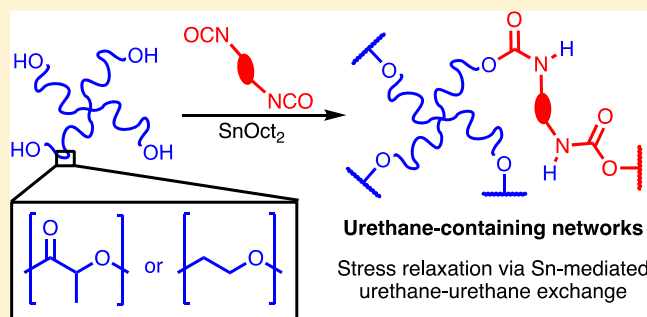
<sup>†</sup>Department of Chemistry, University of Minnesota, 207 Pleasant Street SE, Minneapolis, Minnesota 55455-0431, United States

<sup>‡</sup>Department of Chemistry, Northwestern University, 2145 Sheridan Road, Evanston, Illinois 60208, United States

<sup>§</sup>Department of Chemistry and Chemical Biology, Baker Laboratory, Cornell University, Ithaca, New York 14853, United States

## Supporting Information

**ABSTRACT:** Cross-linked polymers are used in many commercial products and are traditionally incapable of recycling via melt reprocessing. Recently, tough and reprocessable cross-linked polymers have been realized by incorporating cross-links that undergo associative exchange reactions, such as transesterification, at elevated temperatures. Here we investigate how cross-linked polymers containing urethane linkages relax stress under similar conditions, which enables their reprocessing. Materials based on hydroxyl-terminated star-shaped poly(ethylene oxide) and poly((±)-lactide) were cross-linked with methylene diphenyldiisocyanate in the presence of stannous octoate catalyst. Polymers with lower plateau moduli exhibit faster rates of relaxation. Reactions of model urethanes suggest that exchange occurs through the tin-mediated exchange of the urethanes that does not require free hydroxyl groups. Furthermore, samples were incapable of elevated-temperature dissolution in a low-polarity solvent (1,2,4-trichlorobenzene) but readily dissolved in a high-polarity aprotic solvent (DMSO, 24 to 48 h). These findings indicate that urethane linkages, which are straightforward to incorporate, impart dynamic character to polymer networks of diverse chemical composition, likely through a urethane reversion mechanism.



## INTRODUCTION

Cross-linked polymer networks are prevalent in adhesives, composites, and other durable products. Unlike thermoplastics, traditional cross-linked polymer networks are effectively irreparable, cannot be reshaped, and are nonrecyclable through traditional means. Many studies have explored their reprocessing by incorporating dynamic covalent cross-links.<sup>1–6</sup> Early examples relied on thermally reversible moieties such as Diels–Alder cycloadducts, which allowed the materials to depolymerize and be reformed in a new shape.<sup>7,8</sup> Although this approach represented a significant conceptual advance in the reprocessing of cross-linked polymers, the materials often exhibit poor thermal stability and solvent resistance, which limit their potential applications.<sup>9</sup>

A new class of reprocessable polymer networks, termed vitrimers,<sup>10–12</sup> feature cross-links that typically undergo exchange through associative rather than dissociative processes. Vitrimers maintain their cross-linked nature at elevated temperature and/or in the presence of solvents, as demonstrated for polyester epoxy resins containing a Zn(II) transesterification catalyst.<sup>10,13,14</sup> The cured resins were capable of reprocessing and injection molding at 280 °C; however, they only swell in hot solvent (180 °C) rather than dissolving, as is typical for cross-linked polymers. The temperature dependence of the viscosity

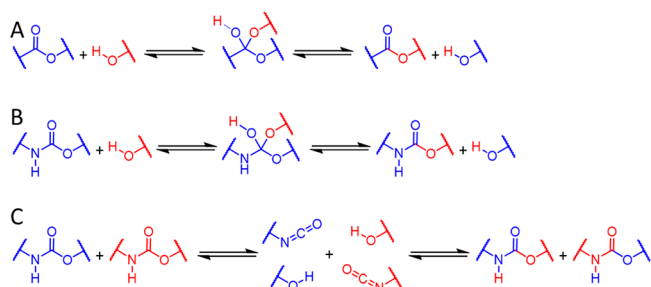
of vitrimers is gradual and follows an Arrhenius relationship, which differs from the typical Williams–Landel–Ferry response observed for thermoplastics. This strong glass-forming behavior confers a topology freezing transition temperature ( $T_v$ ) when it occurs above or at the  $T_g$ . Below  $T_v$ , the vitrimer behaves as a traditional thermoset, and above  $T_v$ , the cross-links undergo dynamic exchange reactions that give rise to thermally activated stress relaxation.

Vitrimers and vitrimer-like materials have been developed on the basis of dynamic chemistry including alkene metathesis,<sup>15,16</sup> hindered urea exchange,<sup>17,18</sup> disulfide/polysulfide metathesis,<sup>19–22</sup> thiol-disulfide exchange,<sup>23</sup> vinylogous urethane exchange,<sup>24,25</sup> transcarbamoylation,<sup>26,27</sup> siloxane equilibrium,<sup>28,29</sup> and boronic ester exchange.<sup>30–32</sup> We previously reported reprocessable materials based on poly((±)-lactide) (PLA) cross-linked with a diisocyanate in the presence of a stannous octoate catalyst.<sup>33</sup> We initially hypothesized that transesterification caused stress relaxation (Scheme 1A) and that the high concentration of ester functionalities in the PLA backbone was responsible for the rapid stress relaxation and efficient

Received: November 28, 2018

Revised: January 15, 2019

### Scheme 1. Proposed Possible Relaxation Mechanisms for Urethane Cross-Linked PLA<sup>a</sup>



<sup>a</sup>(A) Transesterification, (B) transcarbamoylation, and (C) urethane reversion.

reprocessability of these materials. However, the Arrhenius activation energy ( $E_a$ ) for stress relaxation ( $150 \text{ kJ mol}^{-1}$ ) was much higher than that determined for PLA transesterification ( $80 \text{ kJ mol}^{-1}$ ),<sup>34</sup> which indicated that other stress relaxation mechanisms were more likely. We later showed that cross-linked polyhydroxyurethanes relax stress through hydroxyl–urethane exchange (e.g., transcarbamoylation, Scheme 1B),<sup>26,27</sup> suggesting that the urethane linkages might also be responsible for stress relaxation in the PLA networks. Furthermore, stress relaxation of polyurethane networks lacking free hydroxyl groups, which are required for transcarbamoylation, was reported by Tobolsky in the 1950s and was hypothesized to occur via urethane reversion (Scheme 1C).<sup>35,36</sup> Exploiting the dynamic nature of urethane bonds has recently become a promising approach to reshaping polyurethane networks, although mechanistic aspects of these processes are not entirely clear. For example, Zheng et al. hypothesized that urethanes were responsible for stress relaxation in polyurethane elastomers in the presence of dibutyltin dilaurate.<sup>37</sup> Yan et al. further studied the tin-mediated relaxation of polyurethanes and showed preliminary results indicating that this behavior can be correlated to the reprocessability of cross-linked polyurethanes.<sup>38,39</sup> Additional work by Zheng et al. demonstrated that networks based on *N*-aryl urethanes relax stress at elevated temperatures even in the absence of an external catalyst,<sup>40</sup> although no explicit evidence for urethane reversion was presented in any of these systems. Yang and Urban postulated that the repair of cross-linked polyurethanes occurs through the generation of amines upon mechanical failure, which react further with urethanes to form ureas.<sup>41</sup> Although modest changes in the Raman and IR spectra were consistent with this hypothesis, more definitive characterization was not obtained. Considering these findings, a robust understanding of the mechanisms of stress relaxation for urethane-containing polymer networks has not yet been established.

Here we investigate the thermally activated stress relaxation of urethane-containing polymer networks as a function of temperature, catalyst content, and polymer structure. The similarity of  $E_a$  values for the stress relaxation of PLA- and poly(ethylene oxide) (PEO)-based polymers cross-linked with aryl isocyanates indicates that urethane bonds are the dynamic linkages in both networks and further suggests that transesterification-based relaxation is negligible in PLA-derived urethane networks. Exchange studies of urethane model compounds at elevated temperature provide further insight into the mechanism responsible for stress relaxation. Variable-temperature NMR spectroscopy and polymer swelling experiments are consistent

with urethane reversion being the predominant mechanism of stress relaxation in polymer networks cross-linked by *N*-aryl urethanes.

## EXPERIMENTAL SECTION

**Materials.** All reagents were purchased from Sigma-Aldrich (Milwaukee, WI) and were used as received unless otherwise stated. All glassware was held at  $105 \text{ }^\circ\text{C}$  overnight prior to use unless otherwise specified. ( $\pm$ )-Lactide was kindly provided by Altasorb (Piedmont, SC) and used as received. Stannous octoate [ $\text{Sn}(\text{Oct})_2$ ] was purified by vacuum distillation (three times,  $\sim 130\text{--}150 \text{ }^\circ\text{C}$ , ca.  $30\text{--}50 \text{ mTorr}$  argon). Dichloromethane (DCM) and methanol were purchased from Fisher Scientific (Hampton, NH). DCM was purified via a GC-SPS-4-CM glass contour 800-L solvent purification system obtained from Pure Process Technologies (Nashua, NH). Four-arm hydroxyl-terminated PLA and urethane cross-linked PLA were synthesized using a literature procedure; the number-average molar mass ( $M_n$ ) of the prepolymer was determined by  $^1\text{H}$  NMR spectroscopy.<sup>33</sup> Urethane cross-linked PEO was synthesized under the same conditions as for the PLA samples using commercially available pentaerythritol ethoxylate ( $M_n \approx 797 \text{ g mol}^{-1}$ ). PLA and PEO samples are respectively denoted as PLA-*X*-*Y* and PEO-*X*-*Y*, where *X* is the  $M_n$  of the prepolymer ( $\text{kg mol}^{-1}$ ) and *Y* is the cross-linker used: either methylene diphenyl diisocyanate (MDI) or poly(methylene diphenyl diisocyanate) (PMDI). In some cases, a sample was swollen in methanol (details given in the Characterization Methods section) or contained no catalyst, denoted by SM and NC at the end of the sample name, respectively.

**Synthesis of Epoxide Cross-Linked Poly(4-methylcaprolactone).** The 4-methylcaprolactone monomer was synthesized using a literature procedure.<sup>42</sup>  $\text{Sn}(\text{Oct})_2$  (4 mg, 0.025 mol %) was dissolved in toluene (ca. 0.1 mL) and charged in a pressure vessel, along with 4-methylcaprolactone (5 g, 39 mmol) and pentaerythritol (0.073 g, 0.54 mmol). The reaction mixture was held at  $160 \text{ }^\circ\text{C}$  for 3 h, and then succinic anhydride (0.3 g, 3 mmol) was added under  $\text{N}_2$  and stirred for 1 h. The mixture was cooled, dissolved using DCM, and then precipitated into methanol (ca. 10 times the volume of the product solution). The crude polymer was again dissolved in DCM and reprecipitated in hexanes (ca. 10 times the volume of the product solution). The resulting carboxylic acid-terminated poly(4-methylcaprolactone) (P4MCL) was dried under  $\text{N}_2$  for 24 h and then dried under vacuum (20 mTorr) at  $60 \text{ }^\circ\text{C}$  for 72 h; the isolated yield was 76%.  $^1\text{H}$  NMR (500 MHz,  $\text{CDCl}_3$ ;  $25 \text{ }^\circ\text{C}$ )  $\delta$  4.20–4.01 (m, 158 H), 2.64 (m, 16 H), 2.42–2.23 (m, 150 H), 1.74–1.39 (m, 390 H), 0.97–0.87 (m, 240 H).  $M_n = 10.1 \text{ kg mol}^{-1}$ . DSC:  $T_g = -60 \text{ }^\circ\text{C}$ .

P4MCL (1.52 g, 1.0 equiv of COOH groups), triglycidyl isocyanurate (64 mg, 1.0 equiv of epoxide groups), and  $\text{Sn}(\text{Oct})_2$  (6 mg, 2.5 mol % with respect to COOH groups) were dissolved in DCM. The solution was poured into a polypropylene container and allowed to sit for 24 h before being heated under  $\text{N}_2$  at  $120 \text{ }^\circ\text{C}$  for 3 h. The gel percent of the resultant epoxide cross-linked P4MCL network was 95%.

**Representative Synthesis of N–H Model Compounds.** To a flame-dried round-bottomed flask under a nitrogen atmosphere was added alcohol (16.8 mmol) and anhydrous tetrahydrofuran (20 mL). A solution of  $\text{Sn}(\text{Oct})_2$  (130 mg, 0.34 mmol, 2 mol %) dissolved in anhydrous tetrahydrofuran (1 mL) was added, followed by the addition of isocyanate (16.8 mmol) using a syringe. The resulting solution was stirred at room

temperature for 24 h, and solvent was removed at reduced pressure to yield a white solid. The crude solid was purified by chromatography on silica gel using 20% ethyl acetate/hexanes to yield the product.

***N*-Phenyl-*O*-octyl Urethane.** White solid, 82% yield.  $^1\text{H}$  NMR (400 MHz,  $\text{CDCl}_3$ )  $\delta$  7.38 (d,  $J = 8.0$  Hz, 2H), 7.35–7.23 (m, 2H), 7.05 (tt,  $J = 7.1$ , 1.2 Hz, 1H), 6.56 (br s, 1H), 4.16 (t,  $J = 6.7$  Hz, 2H), 1.71–1.63 (m, 2H), 1.43–1.23 (m, 10H), 0.89 (t,  $J = 7.8$  Hz, 3H).  $^{13}\text{C}$  NMR (100 MHz,  $\text{CDCl}_3$ )  $\delta$  153.7, 138.0, 128.9, 123.2, 118.5, 65.4, 31.7, 29.19, 29.15, 28.9, 25.8, 22.6, 14.0. IR (neat, ATR) 3304, 2956, 2920, 2853, 1698, 1599, 1544, 1444, 1236, 1055, 747  $\text{cm}^{-1}$ .

***N*-Tolyl-*O*-decyl Urethane.** White solid, 85% yield.  $^1\text{H}$  NMR (400 MHz,  $\text{CDCl}_3$ )  $\delta$  7.28–7.22 (m, 2H), 7.10 (d,  $J = 8.3$  Hz, 2H), 6.49 (br s, 1H), 4.14 (t,  $J = 6.7$  Hz, 2H), 2.30 (s, 3H), 1.72–1.60 (m, 2H), 1.44–1.24 (m, 14H), 0.92–0.84 (m, 3H).  $^{13}\text{C}$  NMR (100 MHz,  $\text{CDCl}_3$ )  $\delta$  153.8, 135.4, 132.8, 129.4, 118.7, 65.3, 31.9, 29.51, 29.50, 29.27, 29.25, 28.9, 25.8, 22.6, 20.7, 14.1. IR (neat, ATR) 3327, 2919, 2851, 1696, 1596, 1531, 1314, 1235, 1071, 814  $\text{cm}^{-1}$ .

***N*-Tolyl-*O*-(triethyleneglycol monomethyl ether) Urethane.** Colorless oil, 57% yield.  $^1\text{H}$  NMR (400 MHz,  $\text{CDCl}_3$ )  $\delta$  7.25 (d,  $J = 8.6$  Hz, 2H), 7.10 (d,  $J = 8.0$  Hz, 2H), 6.73 (br s, 1H), 4.35–4.28 (m, 2H), 3.78–3.71 (m, 2H), 3.73–3.62 (m, 6H), 3.59–3.52 (m, 2H), 3.38 (s, 3H), 2.30 (s, 3H).  $^{13}\text{C}$  NMR (100 MHz,  $\text{CDCl}_3$ )  $\delta$  153.5, 135.3, 132.7, 129.3, 118.7, 71.8, 70.42, 70.41, 70.40, 69.3, 63.9, 58.8, 20.6. IR (neat, ATR) 3306, 2873, 1727/1709, 1599, 1530, 1315, 1222, 1207, 1102, 1069, 816  $\text{cm}^{-1}$ .

**Representative Synthesis of *N*- $\text{CH}_3$  Model Compounds.** To a flame-dried round-bottomed flask under a nitrogen atmosphere was added urethane model compound (4 mmol) and anhydrous dimethylformamide (15 mL). The mixture was cooled in an ice bath, and sodium hydride (192 mg, 8.0 mmol, 320 mg dispersion in mineral oil) was added, resulting in gas evolution. The resulting mixture was stirred for 10 min, and then iodomethane (1.419 g, 10 mmol, 0.62 mL) was added using a syringe. The resulting mixture was stirred at room temperature for 18 h and then diluted with water (150 mL). This solution was extracted with diethyl ether (200 mL), which was washed with water ( $2 \times 150$  mL), dried over  $\text{MgSO}_4$ , and filtered. Solvent was removed at reduced pressure to yield a colorless oil. The crude oil was purified via chromatography on silica gel using 10% ethyl acetate/hexanes to yield the product.

***N*-Methyl-*N*-phenyl-*O*-octyl Urethane.** Colorless oil, 65% yield.  $^1\text{H}$  NMR (400 MHz,  $\text{CDCl}_3$ )  $\delta$  7.34 (m, 2H), 7.27–7.15 (m, 3H), 4.09 (t,  $J = 6.7$  Hz, 2H), 3.30 (s, 3H), 1.63–1.53 (m, 2H), 1.33–1.22 (m, 10H), 0.88 (t,  $J = 6.8$  Hz, 3H).  $^{13}\text{C}$  NMR (100 MHz,  $\text{CDCl}_3$ )  $\delta$  155.7, 143.4, 128.7, 125.8, 125.6, 65.8, 37.5, 31.7, 29.11, 29.08, 28.8, 25.8, 22.6, 14.0. IR (neat, ATR) 2925, 2855, 1703, 1598, 1498, 1346, 1154, 695  $\text{cm}^{-1}$ .

***N*-Methyl-*N*-tolyl-*O*-decyl Urethane.** Colorless oil, 55% yield.  $^1\text{H}$  NMR (400 MHz,  $\text{CDCl}_3$ )  $\delta$  7.18–7.07 (m, 4H), 4.08 (t,  $J = 6.7$  Hz, 2H), 3.27 (s, 3H), 2.34 (s, 3H), 1.64–1.54 (m, 2H), 1.35–1.23 (m, 14H), 0.89 (t,  $J = 6.9$  Hz, 3H).  $^{13}\text{C}$  NMR (100 MHz,  $\text{CDCl}_3$ )  $\delta$  155.9, 140.8, 135.6, 129.3, 125.6, 65.8, 37.7, 31.9, 29.5, 29.4, 29.3, 29.1, 28.9, 25.8, 22.6, 20.9, 14.0. IR (neat, ATR) 2923, 2854, 1703, 1515, 1343, 1155, 1111, 820, 768  $\text{cm}^{-1}$ .

**Model Alcohol–Urethane Exchange Reaction Analyzed by GC–MS Analysis.** To a vial was added  $\text{Sn}(\text{Oct})_2$  (11.9 mg, 0.03 mmol, 2.5 mol % with respect to urethane), *N*-phenyl-*O*-octyl urethane (293 mg, 1.17 mmol), 1-decanol (1.86

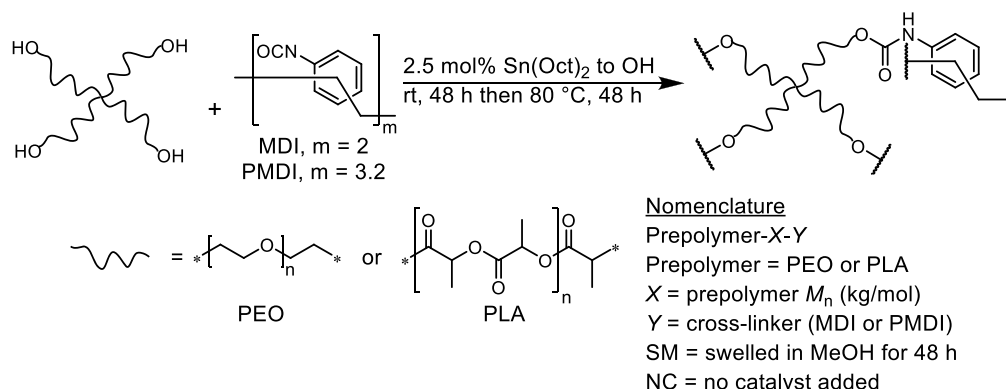
g, 11.7 mmol), and triphenylmethane (27.0 mg, 0.11 mmol) as an internal standard. The resulting mixture was heated and stirred in a preheated oil bath. Aliquots were removed using a syringe at various time points, diluted with DCM, and subjected to GC–MS analysis. Concentrations of the transcarbamoylation product, *N*-phenyl-*O*-decyl urethane, could not be determined quantitatively because of the partial decomposition of the urethanes on the GC column at temperatures required to sufficiently volatilize them.

**Model Alcohol–Urethane Exchange Reaction Analyzed by NMR Spectroscopy.** To a vial was added  $\text{Sn}(\text{Oct})_2$  (11.6 mg, 0.03 mmol, 2.5 mol % with respect to urethane), *N*-tolyl-*O*-(triethyleneglycol monomethyl ether) urethane (340 mg, 1.14 mmol), and 1-decanol (1.81 g, 11.4 mmol). The resulting mixture was then heated and stirred in a preheated oil bath. Aliquots of ca. 10 mg were removed using a syringe at various time points, dissolved in  $\text{CDCl}_3$  (containing 10.0 mg/mL tribromobenzene as an external standard) to a concentration of 50.0 mg/mL, and analyzed by  $^1\text{H}$  NMR spectroscopy (the  $-\text{CH}_2\text{O}-$  peaks of the starting material and transcarbamoylation product are distinct). Concentrations of the transcarbamoylation product, *N*-tolyl-*O*-decyl urethane, could not be determined quantitatively because of the overlap of the product resonance at ca. 4.1 ppm with a side product. (The calculated amount of product formed is greater than the amount of starting material lost. Running the reaction to high conversion clearly shows an overlapping resonance convoluting the product peak.)

**Model Urethane–Urethane Exchange Reaction.** To a vial was added  $\text{Sn}(\text{Oct})_2$  (23.9 mg, 0.059 mmol, 2.5 mol % with respect to urethane), *N*-phenyl-*O*-octyl urethane (294 mg, 1.18 mmol), *N*-tolyl-*O*-decyl urethane (344 mg, 1.18 mmol), and triphenylmethane (30.5 mg, 0.12 mmol) as an internal standard. The resulting mixture was heated and stirred in an oil bath preheated to the desired temperature. Aliquots were removed using a syringe at various time points, diluted with DCM, and subjected to GC–MS analysis. Concentrations of the urethane exchange product, *N*-phenyl-*O*-decyl urethane, could not be determined quantitatively because of the partial decomposition of the urethanes on the GC column at temperatures required to sufficiently volatilize them.

**Synthesis of the Diethyl Urethane Adduct of MDI.** To a round-bottomed flask was added MDI (10 g, 40 mmol), ethanol (9.3 mL, 160 mmol), and DCM (10 mL) with stirring. Once the solution was homogeneous, it was cooled to 0 °C and  $\text{Sn}(\text{Oct})_2$  (0.81 g, 2 mmol, 2.5 mol % with respect to NCO groups) in DCM (10 mL) was added. After 10 min at 0 °C, the solution was left at room temperature for 20 h before concentrating by rotary evaporation and drying under high vacuum ( $\sim 20$  mTorr) for 48 h. The crude product was then dissolved in dimethylformamide (ca. 20 mL) and precipitated into deionized water (ca. 200 mL), yielding a yellow solid that was dried under vacuum (20 mTorr) for 48 h (quantitative yield).  $^1\text{H}$  NMR (500 MHz,  $\text{DMSO}-d_6$ )  $\delta$  9.52 (s, 2H), 7.38 (d, 4H), 7.10 (d, 4H), 4.12 (q, 4H), 3.79 (s, 2H), 1.24 (t, 6H).  $^{13}\text{C}$  NMR (125 MHz,  $\text{DMSO}-d_6$ )  $\delta$  154, 138, 136, 129, 119, 60, 40, 15.

**Characterization Methods.**<sup>26,33,43</sup> NMR spectroscopy was performed on a 500 MHz Bruker Avance III HD with a SampleXpress spectrometer (Billerica, MA) or a 400 MHz Agilent DD MR-400 spectrometer. Solutions were prepared in 99.8%  $\text{CDCl}_3$  (Cambridge Isotope Laboratories). All NMR spectra were acquired at 20 °C with at least 16 scans and a 1 s delay unless otherwise specified. Chemical shifts are reported in

Scheme 2. Synthesis of Urethane Cross-Linked PEOs and PLAs<sup>a</sup>

<sup>a</sup>The bracketed representation for MDI and PMDI is used to show that PMDI is a mixture of regioisomers and oligomers with an average functionality of 3.2 isocyanate groups and an average  $M_n \approx 400$  g/mol.

ppm with respect to residual  $\text{CHCl}_3$  (7.26 ppm). Variable-temperature (VT) NMR was performed on a 500 MHz Bruker III at 100 and 140 °C.  $\text{DMSO-}d_6$  (Cambridge Isotope Laboratories, 99.9%) was purified by distillation over  $\text{CaH}_2$ . The solution for VT-NMR was prepared and sealed in a high-pressure NMR tube under  $\text{N}_2$ . The same solution was allowed to equilibrate at the desired temperature for 10 min before the  $^1\text{H}$  NMR and  $^{13}\text{C}$  NMR spectra were acquired.

FTIR was performed on a Bruker Alpha Platinum with a single-reflection diamond ATR head or a Thermo Nicolet iS10 equipped with a ZnSe ATR attachment. Spectra were obtained from 400 to 4000  $\text{cm}^{-1}$  using a minimum of 16 scans. For each spectrum, the transmission intensity data were normalized with respect to the carbonyl stretch.

Gas chromatography–electron impact mass spectrometry (GC–MS) was performed on an Agilent 6890N Network GC system with a JEOL JMS-GCmate II mass spectrometer (magnetic sector). Triphenylmethane was used as an internal standard.

Dynamic mechanical thermal analysis (DMTA) was performed on a TA Instruments RSA-G2 analyzer (New Castle, DE) using dog-bone-shaped films (ca. 0.5 mm (T)  $\times$  3 mm (W)  $\times$  25 mm (L) and a gauge length of 14 mm). DMTA experiments were conducted in tension film mode, where the axial force was first adjusted to a tension of 0.2 N (sensitivity of 0.01 N) to ensure no buckling of the sample. The proportional force mode was set to force tracking to ensure that the axial force was at least 100% greater than the dynamic oscillatory force. The strain adjust was then set to 30% with a minimum strain of 0.05%, a maximum strain of 5%, and a maximum force of 0.2 N to prevent the sample from going out of the specified strain range. A temperature ramp was then performed from  $-50$  to 200 °C at a rate of 5 °C  $\text{min}^{-1}$ , with an oscillating strain of 0.05% and an angular frequency of 6.28  $\text{rad s}^{-1}$ . PLA samples required a higher starting temperature (25 to 35 °C) because of transducer overload in the glassy regime. The glass-transition temperature ( $T_g$ ) was determined from the maximum value of the loss modulus. The cross-link density ( $\nu_c$ ) and the molar mass between cross-links ( $M_x$ ) were calculated using the storage modulus ( $E'$ ) at 100 °C with eq 1.

$$E'(T) = 3G'(T) = 3RT\nu_c = \frac{3\rho RT}{M_x} \quad (1)$$

where  $G'$  is the storage modulus under shear,  $R$  is the universal gas constant,  $T$  is the absolute temperature in the rubbery region (ca. 373 K), and  $\rho$  is the density of PLA (1.25  $\text{g cm}^{-3}$ ) or PEO (1.13  $\text{g cm}^{-3}$ ).

The stress–relaxation analysis (SRA) experiments were performed under strain control at a specified temperature (110–170 °C depending on the sample). The samples were allowed to equilibrate at a chosen temperature for approximately 10 min, after which the axial force was then adjusted to 0 N with a sensitivity of 0.05 N. Each sample was then subjected to an instantaneous 5% strain. The stress decay was monitored while maintaining a constant strain (5%) until the stress relaxation modulus had relaxed to 37% ( $1/e$ ) of its initial value. The characteristic relaxation time ( $\tau^*$ ), or the time required for the modulus to reach 37% ( $1/e$ ) of its initial value, was measured three times in succession for each sample at each temperature. These points were then plotted versus  $1/T$  and fit to the Arrhenius relationship in eq 2.

$$\tau^*(T) = \tau_0 e^{E_a/RT} \quad (2)$$

where  $\tau_0$  is the characteristic relaxation time at infinite  $T$ ,  $E_a$  is the activation energy of stress relaxation ( $\text{kJ mol}^{-1}$ ),  $R$  is the universal gas constant, and  $T$  is the temperature in K at which SRA was performed.

$T_v$  is defined as the point at which a material exhibits a viscosity of  $10^{12}$  Pa s, also known as the liquid-to-solid transition viscosity ( $\eta_v$ ).<sup>44–46</sup> Using Maxwell's relation (eq 3)<sup>47</sup> and the  $E'$  measured by DMTA at 100 °C, the  $\tau^*$  at  $T_v$  ( $\tau_v^*$ ) was determined for each sample. The Arrhenius fit for each sample was then extrapolated to the corresponding  $\tau_v^*$  to determine  $T_v$ .

$$\eta_v = \frac{1}{3} E' \tau_v^* \quad (3)$$

Differential scanning calorimetry (DSC) was conducted on a TA Instruments Discovery DSC (New Castle, DE). The instrument was calibrated using an indium standard. All samples (ca. 3–7 mg) were analyzed using T-Zero hermetic pans under a  $\text{N}_2$  purge of 50  $\text{mL min}^{-1}$ . The samples were initially cooled to  $-80$  °C and then heated to 150 °C at 10 °C  $\text{min}^{-1}$ . After a 1 min isotherm, the samples were cooled to  $-80$  °C at 10 °C  $\text{min}^{-1}$  and heated again to 150 °C at the same rate. Values for  $T_g$  were acquired at the midpoint of each transition in the second heating curve using Trios software. Thermogravimetric analysis (TGA) was performed on a TA Instruments Q500 (New Castle, DE)

under air at a heating rate of 10 °C/min from room temperature to 550 °C. A typical sample size was between 8 and 15 mg.

Solvent extraction experiments were performed by placing a small amount of cross-linked polymer (ca. 20–100 mg) into a 20 mL vial filled with DCM or MeOH. The vial was then closed and stirred for 48 h before removing the solvent by gravity filtration. The recovered sample was dried under reduced pressure for 48 h at 20 mTorr, after which the sample was weighed and the gel percent was determined. A high-temperature swell test was also performed with PEO-0.8-MDI (with and without catalyst) submerged in 1,2,4-trichlorobenzene (TCB) or anhydrous dimethylsulfoxide (DMSO) at 140 °C for 7 days or until full dissolution occurred.

Trace Sn analysis was performed by Chemical Solutions Ltd. using inductively coupled plasma–mass spectrometry (ICP–MS) after microwave digestion of the samples. Five samples were subjected to trace Sn analysis: PEO-0.8-PMDI (0.44 wt % Sn), PEO-0.8-MDI (0.54 wt % Sn), PEO-0.8-PMDI-SM (0.96 wt % Sn), PEO-0.8-MDI-SM (0.52 wt % Sn), and PEO-0.8-MDI-NC (0.00053 wt % Sn).

## RESULTS AND DISCUSSION

In our previous study of urethane cross-linked PLA,<sup>33</sup> the  $E_a$  of stress relaxation (150 kJ mol<sup>-1</sup>) was far higher than that reported for Sn(Oct)<sub>2</sub>-catalyzed transesterification in a PLA melt (80 kJ mol<sup>-1</sup>).<sup>34</sup> To further investigate, we substituted the PLA component with PEO; if transesterification reactions are the dominant mechanism of stress relaxation, then PEO-based materials would exhibit distinctly different stress relaxation behavior as a result of the lack of ester linkages in PEO. Urethane cross-linked PEO materials were prepared using conditions similar to those used for urethane cross-linked PLA (Scheme 2).<sup>33</sup> The commercially available PEO prepolymer was combined with MDI (NCO functionality of 2, 0.75 NCO group per OH group) and Sn(Oct)<sub>2</sub> (2.5 mol % relative to initial OH groups) to afford cross-linked networks. The cross-link density of the PEO-based materials was varied by using PMDI (average NCO functionality of 3.2, 0.75 NCO group per OH group) as an alternate cross-linker. The NCO/OH ratio was chosen in order to maintain consistency between this study and our previous study.<sup>33</sup> To directly compare these materials with PLA-based polymers, we prepared hydroxyl-terminated, star-shaped PLA prepolymers with  $M_n = 1.0, 3.8, \text{ and } 10 \text{ kg mol}^{-1}$  and cross-linked them under the same conditions as those used for the PEO prepolymers (Scheme 2). Some PEO-based samples were swollen in methanol (MeOH) after curing to study the effect of alcohol treatment on stress relaxation. Similarly, a control PEO-based sample was prepared without catalyst.

DMTA of the PEO-based materials exhibited a plateau modulus of 3.7 MPa for the MDI-based materials and a modulus of 6.6 MPa for those prepared with PMDI, indicating that the higher isocyanate functionality of PMDI increased the cross-link density as expected (Figure 1, Table 1). During the DMTA experiment, an increase in the modulus of the materials with catalyst was observed above 150 °C. After cooling the samples back to room temperature, we subjected them to a second DMTA experiment and found that the plateau moduli had increased slightly (Figure S1). These increases in the moduli are likely the outcome of further cross-linking at  $\geq 150$  °C. By comparison with the DMTA data for materials without catalyst and those swollen in MeOH, it is apparent that the presence of catalyst was necessary to observe further cross-linking at high

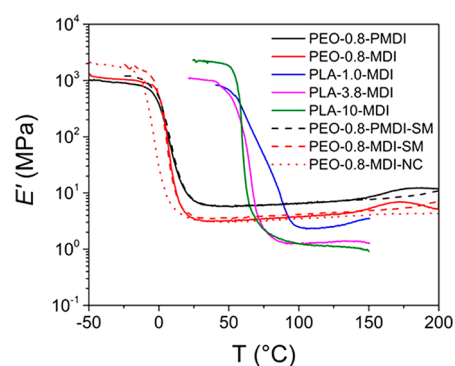


**Figure 1.** DMTA of urethane cross-linked PEO and PLA samples. The dashed lines indicate samples soaked in methanol (SM) and dried under vacuum, and the dotted line indicates the control sample with no catalyst (NC). The analysis was run at 1 Hz with an oscillation strain of 0.05%. PLA samples were tested below 150 °C to avoid thermal decomposition and at higher initial temperatures to avoid transducer overload in the glassy regime.

temperature. Varying the  $M_n$  of the PLA prepolymer affected the plateau modulus as expected: higher  $M_n$  prepolymers yielded less densely cross-linked materials and thus lower plateau moduli. We attributed the similar plateau moduli of PLA-3.8-MDI and PLA-10-MDI to the presence of trapped entanglements, which became more prevalent as the prepolymer  $M_n$  was increased (Figure 1, Table 1). The reported molar mass between entanglements ( $M_e$ ) for PLA is 4 kg mol<sup>-1</sup>, and the critical molar mass ( $M_c$ ) at which entanglements are experimentally observed for PLA is 9 kg mol<sup>-1</sup>,<sup>48</sup> which is consistent with the  $M_x$  of 8.9 kg mol<sup>-1</sup> determined for these samples.

SRA of the PEO-based materials revealed stress relaxation similar to that of PLA-based materials (Figure 2A), suggesting that urethanes, not esters, are the dominant functional groups contributing to stress relaxation. These findings are also consistent with the remarkably slow stress relaxation observed for an aliphatic polyester network containing Sn(Oct)<sub>2</sub> but no urethanes (epoxide cross-linked poly(4-methylcaprolactone), Figure S2). Furthermore, the lack of significant transesterification observed in poly(4-methylcaprolactone) and PLA-based materials is in agreement with a recently reported model compound study using Sn(Oct)<sub>2</sub>: transesterification between benzyl alcohol and a  $\beta$ -lactone was rapid at 120 °C, but no transesterification of the resultant unstrained products was observed after 24 h.<sup>42</sup> The characteristic relaxation times ( $\tau^*$ ) for PEO- and PLA-based materials at various temperatures were fitted to an Arrhenius model (eq 2), from which an  $E_a$  of stress relaxation was extracted (Figure 2B, Table 1). The  $E_a$  did not vary significantly between the PEO- and PLA-based materials containing Sn(Oct)<sub>2</sub> (the range was 139–165 kJ mol<sup>-1</sup>, consistent with our previous work), providing further evidence that the urethane functionality dominates the stress relaxation behavior in all cases. FTIR spectra of all materials before and after SRA are indistinguishable, indicating that the functional groups in the networks are stable at the elevated temperatures employed in this study (Figures S3–S5). Explicitly, we see no formation of common byproducts seen in polyurethanes, such as allophanates, ureas, biurets, and isocyanurates.

While the  $E_a$  values were similar across all polymers studied, the rates of relaxation differed significantly depending on the structure of the networks. Relaxation rates increased dramatically with decreasing plateau modulus (Figure 3), which is

**Table 1. Mechanical and Thermal Data of Urethane Cross-Linked PEOs and PLAs**

sample <sup>a</sup>	gel % <sup>b</sup>	$E'$ (MPa)	$\nu_c \times 10^4$ (mol mL <sup>-1</sup> ) <sup>d</sup>	$M_x$ (kg mol <sup>-1</sup> ) <sup>d</sup>	$T_{g,DMTA}$ (°C) <sup>e</sup>	$T_{g,DSC}$ (°C) <sup>f</sup>	$T_{d,5\%}$ (°C) <sup>g</sup>	$E_a$ (kJ mol <sup>-1</sup> ) <sup>h</sup>	$T_v$ (°C) <sup>i</sup>
PEO-0.8-PMDI	99	6.6	7.1	1.6	3	1	303	142 ± 11	83
PEO-0.8-MDI	100	3.7	4.0	2.8	-1	-3	294	139 ± 5	76
PLA-1-MDI	99	2.4	2.6	4.8	63	55	189	155 ± 5	67
PLA-3.8-MDI	99	1.3	1.4	8.9	54	55	188	153 ± 3	56
PLA-10-MDI	99	1.3	1.4	8.9	53	53	202	165 ± 3	59
PEO-0.8-PMDI-SM	100	6.6	7.1	1.6	0	-1	299	127 ± 31	108
PEO-0.8-MDI-SM	100	4.2	4.5	2.5	0	-4	293	87 ± 27	81
PEO-0.8-MDI-NC	95	3.5	3.8	3	-10	-14	309	102 ± 37	91

<sup>a</sup>Samples are named according to the prepolymer type-molar mass (kg mol<sup>-1</sup>)-cross-linker used. SM denotes the samples swollen in methanol, and NC denotes the sample made without catalyst. <sup>b</sup>Determined as the ratio of the dry mass after a swell test to the mass before the swell test multiplied by 100. <sup>c</sup>Determined at 100 °C. <sup>d</sup>Determined using eq 1. <sup>e</sup>Defined as the temperature where the maximum in the loss modulus ( $E''$ ) occurs in DMTA. <sup>f</sup>Measured after erasing the thermal history at 150 °C for 1 min, cooling to -80 °C, and heating back to 150 °C at a rate 10 °C min<sup>-1</sup>. <sup>g</sup>Determined by heating from 20 to 550 °C under air at 10 °C min<sup>-1</sup>. <sup>h</sup>Determined from the Arrhenius fit from SRA (eq 2). The standard error as determined by Origin software is shown with these values. <sup>i</sup>Determined by extrapolating the Arrhenius fit from SRA to  $\tau_v^*$  for each individual sample, which is determined using eq 3.

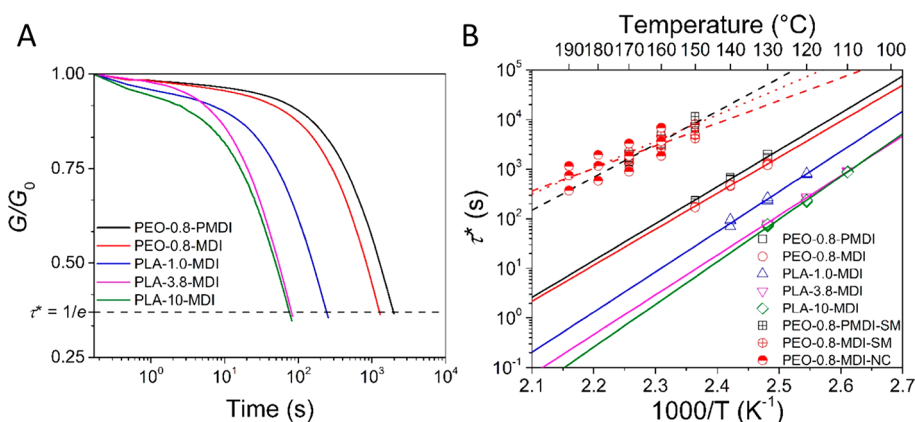


**Figure 2.** (A) SRA for PEO- and PLA-based materials at 130 °C and 5% strain. The experiments were stopped once the sample reached 1/e (37%) of the initial stress relaxation modulus ( $G_0$ ). (B) Arrhenius analyses of the characteristic relaxation times for each sample. Three repetitions at each temperature are plotted. Dashed lines indicate samples that were swollen in MeOH, and the dotted line indicates the sample prepared with no catalyst.

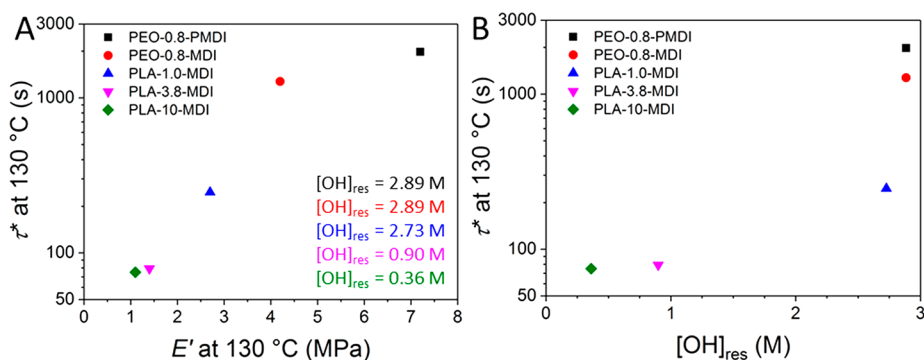


**Figure 3.** Plots of the characteristic relaxation time ( $\tau^*$ ) at 130 °C as a function of (A) the storage modulus ( $E'$ ) at 130 °C and (B)  $[\text{OH}]_{\text{res}}$ , which was estimated from the cross-linking reaction stoichiometry. The values of  $[\text{OH}]_{\text{res}}$  are also shown in A using the color that corresponds to each material.

consistent with previous studies performed on polyester vitrimers.<sup>49</sup> On the basis of stoichiometry, PEO-0.8-PMDI and PEO-0.8-MDI have nearly identical residual hydroxyl group concentrations ( $[\text{OH}]_{\text{res}}$ ); however, the slower stress relaxation behavior of PEO-0.8-PMDI suggested that the modulus influenced the relaxation rate more strongly than did  $[\text{OH}]_{\text{res}}$  (Figure 3). Likewise, PLA-3.8-MDI and PLA-10-MDI had similar plateau moduli and vastly different  $[\text{OH}]_{\text{res}}$  values, yet their rates of stress relaxation were essentially identical (Figure 3). Although it is difficult to completely decouple the influence

of  $E'$  and  $[\text{OH}]_{\text{res}}$  on the stress relaxation rate, it is apparent that across all samples, both in this work and in our previous study, the modulus has a stronger influence on the relaxation rate than the residual hydroxyl concentration.<sup>33</sup> Samples with a lower plateau modulus have a lower urethane concentration, which suggests that the likely mechanism of relaxation is not bimolecular. We speculate that relaxation is more rapid at lower cross-link density because of the increased ability of reactive groups to diffuse within the network. Furthermore, if the mechanism of relaxation were dissociative, each urethane

reversion would have a proportionally greater effect on the reduction of the overall cross-link density in more loosely cross-linked networks.

In our previous studies with PLA-based materials, we found that urethane-based stress relaxation occurred more rapidly in the presence of  $\text{Sn}(\text{Oct})_2$ ,<sup>33</sup> however, we did not determine an  $E_a$  for stress relaxation in the absence of  $\text{Sn}(\text{Oct})_2$ . Therefore, we investigated the stress relaxation of PEO-based materials prepared without a catalyst as well as catalyst-containing materials that had been swollen in MeOH. The rate of relaxation was approximately 30 times slower in the absence of  $\text{Sn}(\text{Oct})_2$  (Figure 2B, dotted line), indicating that the presence of tin greatly facilitates stress relaxation. We observed similar slow relaxation behavior in the samples swollen in MeOH (PEO-0.8-MDI-SM and PEO-0.8-PMDI-SM, Figure 2B, dashed lines). Although we initially hypothesized that MeOH treatment would completely remove the catalyst, the Sn contents of samples pre- and postswelling were evaluated by ICP-MS and determined to be between 0.4 and 1 wt %, which indicated that Sn was not effectively removed by swelling the samples in MeOH. The Sn content of a sample prepared without catalyst was negligible (<1 ppm). Therefore, the ICP-MS and SRA results suggest that swelling in excess MeOH possibly deactivates the  $\text{Sn}(\text{Oct})_2$  catalyst toward urethane exchange rather than removing it. For the MeOH-treated and catalyst-free samples, the  $\tau^*$  values increased significantly after each successive run at a given temperature, resulting in large errors for the calculated activation energies. There were no evident changes in the FTIR spectra before and after SRA for these samples, and no significant mass loss observed before 290 °C (Figures S5 and S15). However, SRA resulted in discoloration of the samples, and we suspect that the inconsistent stress relaxation behavior between successive runs was at least partially due to the decomposition of the reactive functionalities or the formation of additional non-dynamic cross-links. The multiple processes contributing to stress relaxation in the absence of active tin species convolute the comparison of the measured activation energies between MeOH-treated and catalyst-free samples and those with  $\text{Sn}(\text{Oct})_2$  present.

To further understand the exchange reactions of urethanes and the effects of hydroxyl groups on these processes, we studied the behavior of urethane-containing model compounds at elevated temperature. In the presence of excess 1-decanol and  $\text{Sn}(\text{Oct})_2$  (2.5 mol % with respect to urethane) at 150 °C, *N*-phenyl-*O*-octyl urethane reacted to yield the *O*-decyl urethane at a much slower rate compared to the timescale of the stress relaxation (Figure 4A). We therefore analyzed the reaction between two discrete urethanes in the absence of exogenous alcohol (Figure 4B). Under these conditions, the formation of crossover products is observed more quickly and at timescales more similar to stress relaxation, suggesting that urethane reversion, not alcohol-induced associative exchange, is the dominant exchange mechanism (Figure 4B). Furthermore, when two discrete urethanes were heated in the presence of exogenous alcohol, only exchange with the free alcohol was observed (at a rate similar to urethane-hydroxyl exchange) (Figure S6A). These results indicate that excess free alcohols trap the isocyanate intermediates that would otherwise enable urethane-urethane exchange. However, the free alcohols also slow the rate of exchange by coordinating to the Sn atoms, thereby attenuating their ability to catalyze urethane exchange. Decreasing the concentration of free alcohol in this model exchange reaction leads to a recovery of the reactivity, consistent

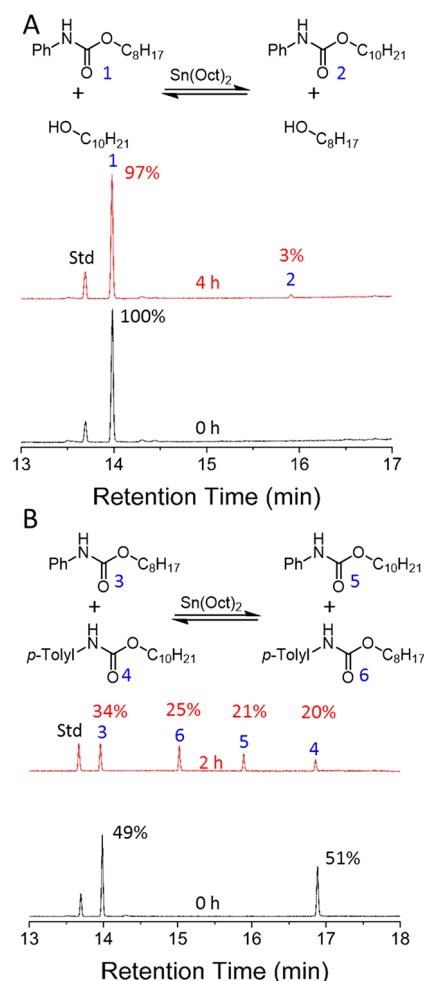


**Figure 4.** GC-MS of model compound studies. (A) Urethane-hydroxyl exchange conducted at 150 °C for 4 h (10 OH groups per urethane) and (B) urethane-urethane exchange performed at 150 °C for 2 h (equimolar in both urethanes). Peak intensities are normalized to triphenylmethane (retention time = 13.7 min). Relative area percentages of each compound are shown, and although qualitatively significant, compound degradation on the GC column prevented quantitative determination (see Figure S6 for more information).

with this interpretation (Figure S7). These findings are consistent with the slower stress relaxation observed for the MeOH-treated samples because while Sn atoms are still present, the rates of relaxation are similar to that of the catalyst-free material.

A urethane-urethane crossover experiment was also conducted on analogous *N*-methylated urethanes to explore the possibility of a distinct metathesis mechanism (Figure S6B) because *N,N*-disubstituted urethanes are incapable of reversion.<sup>26,50</sup> Neither exchange products nor byproducts were observed, again supporting a dissociative urethane exchange mechanism for the nonmethylated urethanes. Unfortunately, the GC-MS results for all model studies were not amenable to quantitative reaction rate determination due to partial decomposition on the GC column (see Figure S6 for more information). Attempts to use <sup>1</sup>H NMR spectroscopy as an alternative method to quantitatively determine the rate of reaction of a free alcohol with a model urethane were complicated by side reactions occurring at the higher temperatures required for hydroxyl-urethane exchange (see Figure S8 for more information).

Although it appeared that a urethane reversion pathway was operative in these systems, this mechanism was inconsistent with the insolubility of these networks in TCB at 140 °C.<sup>33</sup> Other reprocessable cross-linked polymers based on reversible reactions, such as Diels–Alder cycloadditions, are capable of full dissolution at elevated temperatures.<sup>9</sup> Therefore, we posited that the low polarity of TCB was not appropriate for dissolving the polymers but that a polar aprotic solvent such as DMSO could favor dissolution. Indeed, all three variations of PEO-0.8-MDI as well as PLA-1.0-MDI were insoluble in TCB but dissolved fully in anhydrous DMSO at elevated temperature (Figures S9 and S10). Model urethane–urethane exchange studies performed with the addition of DMSO and TCB show very similar reactivity, suggesting that the samples dissolve in DMSO due to the increased swellability or solubility of the samples in DMSO rather than a significant difference in the reactivity of the urethane functional groups (Figure S12). The samples swollen in TCB were dried under vacuum and analyzed using FTIR spectroscopy. While there were some minor detectable differences, no significant change in the carbonyl resonances was observed despite substantial discoloration (Figure S11). In contrast to our expectations based on rates of stress relaxation, the samples treated with MeOH dissolved in DMSO significantly faster (24 h) than samples with (36 h) and without catalyst (48 h to be mostly dissolved, 96 h for complete dissolution). We hypothesize that the additional alcohols in the MeOH-treated samples result in a more rapid net loss of cross-links during the swelling experiment.

Because DMSO was capable of completely dissolving the PEO-based samples, we sought to directly detect the formation of the isocyanate intermediates. We acquired a <sup>13</sup>C NMR spectrum of the diethyl urethane adduct of MDI in DMSO-*d*<sub>6</sub> at 25, 100, and 140 °C (Figure 5). No peaks were observed in the <sup>13</sup>C NMR spectrum that corresponded to the isocyanate, suggesting that the equilibrium significantly favored the urethane at these temperatures. A <sup>1</sup>H NMR spectrum showed only

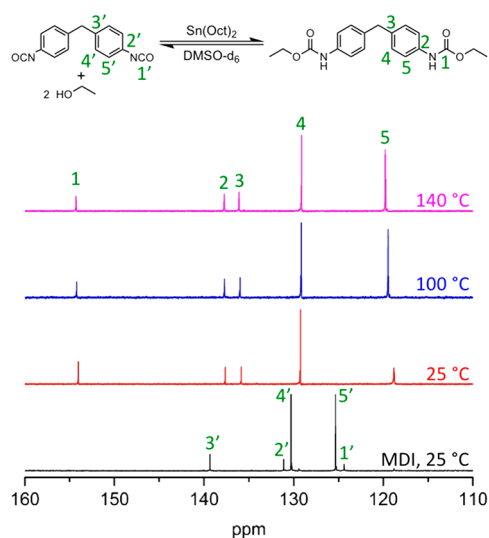


**Figure 5.** <sup>13</sup>C VT-NMR spectra (125 MHz, DMSO-*d*<sub>6</sub>) of MDI and the diethyl urethane adduct of MDI; concentrations of approximately 100 mg mL<sup>-1</sup> were used to achieve a better signal-to-noise ratio. The diethyl urethane solution was under a N<sub>2</sub> atmosphere and contained Sn(Oct)<sub>2</sub> (2.5 mol % with respect to urethanes); the solution was allowed to equilibrate at the desired temperature for 10 min before 128 scans were collected.

an upfield shift of the N–H peak due to the loss of hydrogen bonding (Figure S13), indicating that the isocyanate concentration at these temperatures is below the detection limit of NMR spectroscopy. The fact that urethane is strongly favored at equilibrium at these temperatures is consistent with the Arrhenius-type dependence of stress relaxation because the cross-links never dissociate to the degree required to cause a rapid drop in viscosity.

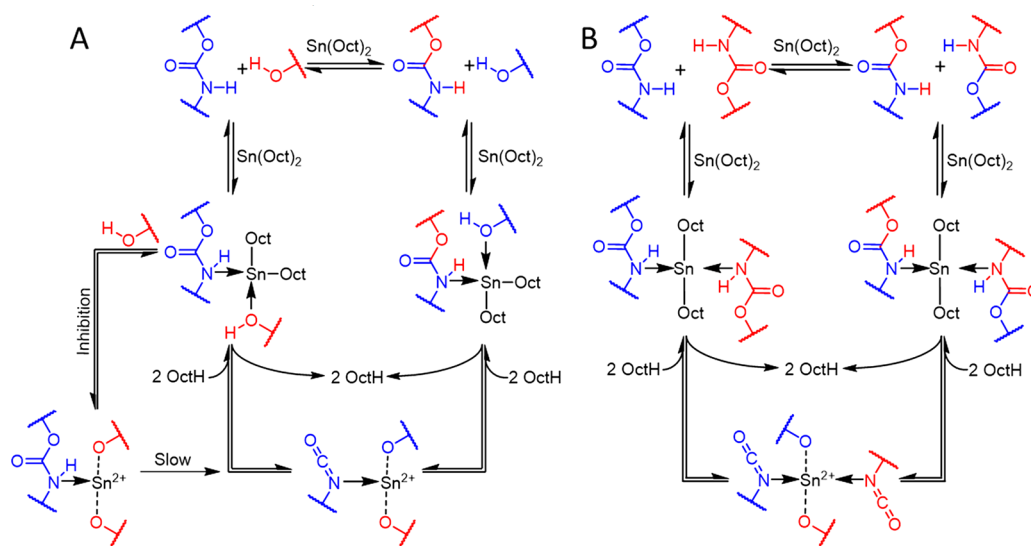
We sought other evidence for a reversion mechanism by indirectly detecting isocyanate-derived species upon removal of alcohol. A mixture of the diethyl urethane adduct of MDI and Sn(Oct)<sub>2</sub> (2.5 mol % with respect to urethane) was heated in a distillation apparatus to drive the formation of MDI by the removal of ethanol. We found that no ethanol was recovered after 24 h at 140 or 150 °C. At 160 °C, however, some ethanol was recovered (18% of the theoretical amount), and we observed an insoluble brown solid in the distillation pot. The FTIR spectrum of the solid indicated the presence of isocyanurate moieties (1509, 1411, and 1171 cm<sup>-1</sup>, Figure S14),<sup>51</sup> which is consistent with the formation of isocyanates followed by trimerization to isocyanurates during alcohol removal. This experiment confirmed that the isocyanate species was transient at temperatures relevant to stress relaxation (140–150 °C), but is consistent with a reversion-based mechanism.

On the basis of SRA, model reactions, and literature precedent,<sup>52,53</sup> we propose two potential mechanisms of stress relaxation in these materials (Scheme 3). In the presence of exogenous alcohol, the mechanism in Scheme 3A would predominate. Low conversion observed in the hydroxyl–urethane exchange model reactions (10 OH groups per urethane) and low relaxation rates in the MeOH-treated samples may arise from the coordination of the Sn(II) metal center by alcohols, inhibiting its ability to catalyze urethane reversion. However, rates would increase as [OH] decreases, which is consistent with the fast urethane–urethane exchange observed in the absence of exogenous alcohol. Furthermore, because [OH]<sub>res</sub> in the cross-linked materials is low, inhibition of the Sn(II) centers by excess alcohol is less likely to occur. Meanwhile, in the absence of exogenous alcohol, urethanes can more freely bind to the catalytic Sn(II) center, allowing for full reversion and subsequently fast exchange (Scheme 3B). This mechanism is consistent with previous observations of polyurethane stress relaxation in both the presence<sup>37,38</sup> and absence<sup>35,36,40</sup> of tin catalysts.

## CONCLUSIONS

We demonstrate that PEO- and PLA-based networks with urethane cross-links are capable of stress relaxation at elevated temperature, likely by urethane reversion. The modulus of the materials is apparently the principal factor controlling the relaxation time, as samples with lower moduli relax more quickly. Although an increase in the concentration of residual hydroxyl moieties slightly lowers the *E*<sub>a</sub> of stress relaxation, [OH]<sub>res</sub> in these materials does not affect the overall rate of relaxation as significantly as the storage modulus, suggesting that reversion is the primary mechanism for urethane exchange. Urethane reversion is further supported by model compound studies in which rapid urethane exchange is observed in the absence of free hydroxyl groups and only when the urethane contains N–H as opposed to N–Me. Furthermore, the alcohol-based inhibition of the Sn(Oct)<sub>2</sub> catalyst is apparent in samples treated with MeOH as well as in model compound reactions performed in a large excess of exogenous alcohol. Although we

**Scheme 3. Proposed Stress Relaxation Mechanisms of (A) the Hydroxyl-Urethane Exchange (Urethane Reversion and Reaction with a New Hydroxyl) and (B) the Urethane–Urethane Exchange (Urethane Reversion and Recombination)<sup>4a</sup>**



<sup>a</sup>Stress relaxation by mechanism A is much slower than by mechanism B due to the competitive inhibition from free hydroxyl groups coordinating to the tin center.

were unable to directly observe the presence of isocyanates using NMR spectroscopy at elevated temperatures, the generation of isocyanurate moieties after the distillation of ethanol from the diethyl urethane adduct of MDI provided further indirect evidence of the formation of isocyanate intermediates. These studies yield insight into the vitrimer-like behavior of polyurethane networks at elevated temperatures and suggest that further investigations of the reprocessability of commercially ubiquitous cross-linked polyurethanes will be a beneficial approach to their recycling.

## ■ ASSOCIATED CONTENT

### Supporting Information

The Supporting Information is available free of charge on the ACS Publications website at DOI: 10.1021/acs.jpcc.8b11489.

SRA, FTIR, GC, TGA, DSC, and <sup>1</sup>H NMR results and pictures of the high-temperature swelling experiments (PDF)

## ■ AUTHOR INFORMATION

### Corresponding Authors

\*E-mail: wdichtel@northwestern.edu.

\*E-mail: hillmyer@umn.edu. Phone: 612-625-7834.

### ORCID

David J. Fortman: 0000-0002-0422-3733

Guilhem X. De Hoe: 0000-0002-0996-7491

William R. Dichtel: 0000-0002-3635-6119

Marc A. Hillmyer: 0000-0001-8255-3853

### Notes

The authors declare no competing financial interest.

## ■ ACKNOWLEDGMENTS

The authors acknowledge the Center for Sustainable Polymers at the University of Minnesota, a National Science Foundation-supported center for chemical innovation (CHE-1413862), for

supporting this work. We also thank Dr. Letitia Yao for performing VT-NMR experiments.

## ■ REFERENCES

- (1) Wu, D. Y.; Meure, S.; Solomon, D. Self-healing Polymeric Materials: A Review of Recent Developments. *Prog. Polym. Sci.* **2008**, *33*, 479–522.
- (2) Tyagi, P.; Deratani, A.; Quemener, D. Self-Healing Dynamic Polymeric Systems. *Isr. J. Chem.* **2013**, *53*, 53–60.
- (3) Kloxin, C. J.; Bowman, C. N. Covalent Adaptable Networks: Smart, Reconfigurable and Responsive Network Systems. *Chem. Soc. Rev.* **2013**, *42*, 7161–7173.
- (4) Wool, R. P. Self-healing Materials: A Review. *Soft Matter* **2008**, *4*, 400–418.
- (5) Wojtecki, R. J.; Meador, M. A.; Rowan, S. J. Using the Dynamic Bond to Access Macroscopically Responsive Structurally Dynamic Polymers. *Nat. Mater.* **2011**, *10*, 14–27.
- (6) Roy, N.; Bruchmann, B.; Lehn, J.-M. DYNAMERS: Dynamic Polymers as Self-healing Materials. *Chem. Soc. Rev.* **2015**, *44*, 3786–3807.
- (7) Chen, X.; Dam, M. A.; Ono, K.; Mal, A.; Shen, H.; Nutt, S. R.; Sheran, K.; Wudl, F. A Thermally Re-mendable Cross-Linked Polymeric Material. *Science* **2002**, *295*, 1698–1702.
- (8) Chen, X.; Wudl, F.; Mal, A. K.; Shen, H.; Nutt, S. R. New Thermally Remendable Highly Cross-Linked Polymeric Materials. *Macromolecules* **2003**, *36*, 1802–1807.
- (9) Zhang, Y.; Broekhuis, A. A.; Picchioni, F. Thermally Self-Healing Polymeric Materials: The Next Step to Recycling Thermoset Polymers? *Macromolecules* **2009**, *42*, 1906–1912.
- (10) Montarnal, D.; Capelot, M.; Tournilhac, F.; Leibler, L. Silica-Like Malleable Materials from Permanent Organic Networks. *Science* **2011**, *334*, 965–968.
- (11) Imbernon, L.; Norvez, S. From Landfilling to Vitrimer Chemistry in Rubber Life Cycle. *Eur. Polym. J.* **2016**, *82*, 347–376.
- (12) Denissen, W.; Winne, J. M.; Du Prez, F. E. Vitrimers: Permanent Organic Networks With Glass-like Fluidity. *Chem. Sci.* **2016**, *7*, 30–38.
- (13) Capelot, M.; Montarnal, D.; Tournilhac, F.; Leibler, L. Metal-Catalyzed Transesterification for Healing and Assembling of Thermosets. *J. Am. Chem. Soc.* **2012**, *134*, 7664–7667.

- (14) Capelot, M.; Unterlass, M. M.; Tournilhac, F.; Leibler, L. Catalytic Control of the Vitrimer Glass Transition. *ACS Macro Lett.* **2012**, *1*, 789–792.
- (15) Lu, Y.-X.; Tournilhac, F.; Leibler, L.; Guan, Z. Making Insoluble Polymer Networks Malleable via Olefin Metathesis. *J. Am. Chem. Soc.* **2012**, *134*, 8424–8427.
- (16) Lu, Y.-X.; Guan, Z. Olefin Metathesis for Effective Polymer Healing via Dynamic Exchange of Strong Carbon–Carbon Double Bonds. *J. Am. Chem. Soc.* **2012**, *134*, 14226–14231.
- (17) Ying, H.; Zhang, Y.; Cheng, J. Dynamic Urea Bond for the Design of Reversible and Self-Healing Polymers. *Nat. Commun.* **2014**, *5*, 3218–3227.
- (18) Zhang, Y.; Ying, H.; Hart, K. R.; Wu, Y.; Hsu, A. J.; Coppola, A. M.; Kim, T. A.; Yang, K.; Sottos, N. R.; White, S. R.; Cheng, J. Malleable and Recyclable Poly(urea-urethane) Thermosets Bearing Hindered Urea Bonds. *Adv. Mater.* **2016**, *28*, 7646–7651.
- (19) Martin, R.; Rekondo, A.; Ruiz de Luzuriaga, A.; Cabanero, G.; Grande, H. J.; Odriozola, I. The Processability of a Poly(urea-urethane) Elastomer Reversibly Crosslinked With Aromatic Disulfide Bridges. *J. Mater. Chem. A* **2014**, *2*, 5710–5715.
- (20) Rekondo, A.; Martin, R.; Ruiz de Luzuriaga, A.; Cabanero, G.; Grande, H. J.; Odriozola, I. Catalyst-free Room-temperature Self-healing Elastomers Based on Aromatic Disulfide Metathesis. *Mater. Horiz.* **2014**, *1*, 237–240.
- (21) Xiang, H. P.; Qian, H. J.; Lu, Z. Y.; Rong, M. Z.; Zhang, M. Q. Crack Healing and Reclaiming of Vulcanized Rubber by Triggering the Rearrangement of Inherent Sulfur Crosslinked Networks. *Green Chem.* **2015**, *17*, 4315–4325.
- (22) Xiang, H. P.; Rong, M. Z.; Zhang, M. Q. Self-healing, Reshaping, and Recycling of Vulcanized Chloroprene Rubber: A Case Study of Multitask Cyclic Utilization of Cross-linked Polymer. *ACS Sustainable Chem. Eng.* **2016**, *4*, 2715–2724.
- (23) Pepels, M.; Filot, I.; Klumperman, B.; Goossens, H. Self-healing Systems Based on Disulfide-thiol Exchange Reactions. *Polym. Chem.* **2013**, *4*, 4955–4965.
- (24) Denissen, W.; Rivero, G.; Nicolay, R.; Leibler, L.; Winne, J. M.; Du Prez, F. E. Vinylous Urethane Vitrimers. *Adv. Funct. Mater.* **2015**, *25*, 2451–2457.
- (25) Denissen, W.; Droesbeke, M.; Renaud, N.; Leibler, L.; Winne, J. M.; Du Prez, F. Chemical Control of the Viscoelastic Properties of Vinylous Urethane Vitrimers. *Nat. Commun.* **2017**, *8*, 14857.
- (26) Fortman, D. J.; Brutman, J. P.; Cramer, C. J.; Hillmyer, M. A.; Dichtel, W. R. Mechanically Activated, Catalyst-Free Polyhydroxyurethane Vitrimers. *J. Am. Chem. Soc.* **2015**, *137*, 14019–14022.
- (27) Fortman, D. J.; Brutman, J. P.; Hillmyer, M. A.; Dichtel, W. R. Structural Effects on the Reprocessability and Stress relaxation of Cross-linked Polyhydroxyurethanes. *J. Appl. Polym. Sci.* **2017**, *134*, 44984.
- (28) Zheng, P.; McCarthy, T. J. A Surprise from 1954: Siloxane Equilibration Is a Simple, Robust, and Obvious Polymer Self-Healing Mechanism. *J. Am. Chem. Soc.* **2012**, *134*, 2024–2027.
- (29) Schmolke, W.; Perner, N.; Seiffert, S. Dynamically Cross-Linked Polydimethylsiloxane Networks with Ambient-Temperature Self-Healing. *Macromolecules* **2015**, *48*, 8781–8788.
- (30) Cash, J. J.; Kubo, T.; Bapat, A. P.; Sumerlin, B. S. Room-Temperature Self-Healing Polymers Based on Dynamic-Covalent Boronic Esters. *Macromolecules* **2015**, *48*, 2098–2106.
- (31) Cromwell, O. R.; Chung, J.; Guan, Z. Malleable and Self-Healing Covalent Polymer Networks through Tunable Dynamic Boronic Ester Bonds. *J. Am. Chem. Soc.* **2015**, *137*, 6492–6495.
- (32) Roettger, M.; Domenech, T.; van der Weegen, R.; Breuillac, A.; Renaud, N.; Leibler, L. High-performance Vitrimers from Commodity Thermoplastics through Dioxaborolane Metathesis. *Science* **2017**, *356*, 62–65.
- (33) Brutman, J. P.; Delgado, P. A.; Hillmyer, M. A. Polylactide Vitrimers. *ACS Macro Lett.* **2014**, *3*, 607–610.
- (34) Yu, Y.; Storti, G.; Morbidelli, M. Kinetics of Ring-Opening Polymerization of L-Lactide. *Ind. Eng. Chem. Res.* **2011**, *50*, 7927–7940.
- (35) Colodny, P. C.; Tobolsky, A. V. Chemorheological Study of Polyurethane Elastomers. *J. Am. Chem. Soc.* **1957**, *79*, 4320–4323.
- (36) Offenbach, J. A.; Tobolsky, A. V. Chemical Relaxation of Stress in Polyurethane Elastomers. *J. Colloid Sci.* **1956**, *11*, 39–47.
- (37) Zheng, N.; Fang, Z.; Zou, W.; Zhao, Q.; Xie, T. Thermoset Shape-Memory Polyurethane with Intrinsic Plasticity Enabled by Transcarbamoylation. *Angew. Chem., Int. Ed.* **2016**, *55*, 11421–11425.
- (38) Yan, P.; Zhao, W.; Fu, X.; Liu, Z.; Kong, W.; Zhou, C.; Lei, J. Multifunctional Polyurethane-Vitrimers Completely Based on Transcarbamoylation of Carbamates: Thermally-Induced Shape Memory Effect and Self-Welding. *RSC Adv.* **2017**, *7*, 26858–26866.
- (39) Yan, P.; Zhao, W.; Wang, Y.; Jiang, Y.; Zhou, C.; Lei, J. Carbon Nanotubes-Polyurethane Vitrimer Nanocomposites with the Ability of Surface Welding Controlled by Heat and Near-Infrared Light. *Macromol. Chem. Phys.* **2017**, *218*, 1700265.
- (40) Zheng, N.; Hou, J.; Xu, Y.; Fang, Z.; Zou, W.; Zhao, Q.; Xie, T. Catalyst-Free Thermoset Polyurethane with Permanent Shape Reconfigurability and Highly Tunable Triple-Shape Memory Performance. *ACS Macro Lett.* **2017**, *6*, 326–330.
- (41) Yang, Y.; Urban, M. W. Self-Healing of Glucose-Modified Polyurethane Networks Facilitated by Damage-Induced Primary Amines. *Polym. Chem.* **2017**, *8*, 303–309.
- (42) De Hoe, G. X.; Zumstein, M. T.; Tiegs, B. J.; Brutman, J. P.; McNeill, K.; Sander, M.; Coates, G. W.; Hillmyer, M. A. Sustainable Polyester Elastomers from Lactones: Synthesis, Properties, and Enzymatic Hydrolyzability. *J. Am. Chem. Soc.* **2018**, *140*, 963–973.
- (43) Brutman, J. P.; De Hoe, G. X.; Schneiderman, D. K.; Le, T. N.; Hillmyer, M. A. Renewable, Degradable, and Chemically Recyclable Cross-Linked Elastomers. *Ind. Eng. Chem. Res.* **2016**, *55*, 11097–11106.
- (44) Angell, C. A. Formation of Glasses from Liquids and Biopolymers. *Science* **1995**, *267*, 1924–1935.
- (45) Ediger, M. D.; Angell, C. A.; Nagel, S. R. Supercooled Liquids and Glasses. *J. Phys. Chem.* **1996**, *100*, 13200–13212.
- (46) Dyre, J. C. *Colloquium: The Glass Transition and Elastic Models of Glass-forming Liquids.* *Rev. Mod. Phys.* **2006**, *78*, 953–972.
- (47) Hiemenz, P. C.; Lodge, T. P. *Polymer Chemistry*, 2nd ed.; CRC Press: Boca Raton, FL, 2007.
- (48) Auras, R. A.; Lim, L. T.; Selke, S. E. M.; Tsuji, H. *Poly(lactic acid): Synthesis, Structures, Properties, Processing, and Applications*; John Wiley & Sons: Hoboken, NJ, 2010.
- (49) Yu, K.; Taynton, P.; Zhang, W.; Dunn, M. L.; Qi, H. J. Influence of Stoichiometry on the Glass Transition and Bond Exchange Reactions in Epoxy Thermoset Polymers. *RSC Adv.* **2014**, *4*, 48682–48690.
- (50) Gaylord, N. G.; Sroog, C. E. The Reactions of Carbamates with Alcohols. *J. Org. Chem.* **1953**, *18*, 1632–1637.
- (51) Pawar, G. M.; Buchmeiser, M. R. Polymer-Supported, Carbon Dioxide-Protected N-Heterocyclic Carbenes: Synthesis and Application in Organo- and Organometallic Catalysis. *Adv. Synth. Catal.* **2010**, *352*, 917–928.
- (52) Bloodworth, A. J.; Davies, A. G. Organometallic Reactions. Part I. The Addition of Tin Alkoxides to Isocyanates. *J. Chem. Soc.* **1965**, 5238–5244.
- (53) Delebecq, E.; Pascault, J.-P.; Boutevin, B.; Ganachaud, F. On the Versatility of Urethane/Urea Bonds: Reversibility, Blocked Isocyanate, and Non-isocyanate Polyurethane. *Chem. Rev.* **2013**, *113*, 80–118.